Tao, Jin; Du, Lei; Dehmer, Matthias; Wen, Yuanqiao; Xie, Guangming; Zhou, Quan

# Path following control for towing system of cylindrical drilling platform in presence of disturbances and uncertainties

*Published in:*
ISA Transactions

*DOI:*
10.1016/j.isatra.2019.04.030

Published: 01/01/2019

*Document Version*
Peer-reviewed accepted author manuscript, also known as Final accepted manuscript or Post-print

*Published under the following license:*
Unspecified

*Please cite the original version:*
Tao, J., Du, L., Dehmer, M., Wen, Y., Xie, G., & Zhou, Q. (2019). Path following control for towing system of cylindrical drilling platform in presence of disturbances and uncertainties. *ISA Transactions*, *95*, 185-193. https://doi.org/10.1016/j.isatra.2019.04.030

# Accepted Manuscript


Path following control for towing system of cylindrical drilling platform in presence of disturbances and uncertainties

Jin Tao, Lei Du, Matthias Dehmer, Yuanqiao Wen, Guangming Xie, Quan Zhou

PII: S0019-0578(19)30204-6
DOI: https://doi.org/10.1016/j.isatra.2019.04.030
Reference: ISATRA 3190

To appear in: *ISA Transactions*

Received date : 11 January 2019
Revised date : 24 April 2019
Accepted date : 26 April 2019

# Authors list

Jin Tao (Corresponding author), Academy Postdoctoral Researcher

Department of Electrical Engineering and Automation, Aalto University, Espoo, Finland

College of Engineering, Peking University, Beijing, China

Tel.: +358-44-9157479

E-mail: jin.tao@aalto.fi

Lei Du, Doctoral Candidate

Department of Mechanical Engineering, Aalto University, Espoo, Finland

Matthias Dehmer, Professor

University of Applied Sciences Upper Austria

Nankai University, Tianjin, China

Yuanqiao Wen, Professor

School of Navigation, Wuhan University of Technology, Wuhan, China

Guangming Xie, Professor

College of Engineering, Peking University, Beijing, China

Quan Zhou, Professor

Department of Electrical Engineering and Automation, Aalto University, Espoo, Finland

**Acknowledgements**

The work was sponsored by Academy of Finland under grant No. 315660.

# Path following control for towing system of cylindrical drilling platform in presence of disturbances and uncertainties

**Abstract**

Towing is a critical process to deploy a cylindrical drilling platform. However, the towing process faces a great variety of risks from a complex nautical environment, the dynamics in towing and maneuvering, to unexpected events. Therefore, safely navigating the towing system following a planned route to a target sea area is essential. To tackle the time-varying disturbances induced by wind, current and system parametric uncertainties, a path following control method for a towing system of cylindrical drilling platform is designed based on linear active disturbance rejection control. By utilizing Maneuvering Modeling Group model as well as a catenary model, we develop a three degree-of-freedom dynamic mathematical model of the towing system under external environmental disturbances and internal uncertainties. Furthermore, we design a linear active disturbance rejection control path following controller for real-time tracking error correction based on a guidance method combining cross-track error and parallax. Finally, the path following performance of the towing system is evaluated in a simulation environment under various disturbances and internal uncertainties, where the corresponding tracking error is analyzed. The results show that the linear active disturbance rejection control performs well under both the external disturbance and inherent uncertainties, and better satisfy the tracking performance criteria than a traditional proportional integral derivative controller.

*Keywords:* towing system, cylindrical drilling platform, path following control, linear active disturbance rejection control, proportionalintegralderivative, disturbances and uncertainties

## 1. Introduction

The ocean is rich in energy resources such as oil, gas and minerals, which can effectively alleviate the global resource and energy crisis [1, 2]. Many countries have paid much attention to deep-ocean oil exploration and development. For example, the Chinese national development strategy taking place from 2014 to 2020 calls for strengthening deep-sea oil and gas exploitation aiming to promote their production vigorously [3]. Consequently, such demand for exploration of new energy resource leads to increasingly wide deployment of offshore drilling platforms [4]. Cylindrical drilling platform is the most advanced mobile oil platform. Due to its stability and reliability, it can deal with well harsh ocean environments [5]. The towing process is the necessary preparation step for the deployment of the platform, where the process faces a great variety of risks from a complex nautical environment, the dynamics in towing and maneuvering, to unexpected events during the operation. Currently, offshore towing operations mainly rely on human dispatching and command, where the human factor is the primary cause of ship accidents [6]. Therefore, intelligent dispatching and control are highly desired, which can lead to safer navigation. For the towing process, it is, therefore, necessary to introduce intelligent control methods to improve the stability of the towing process [7, 8].

In practice, offshore towing is always pre-planned. The towing operating area, where the water depth suffices, usually restricts other ships from passing. However, a towing system, usually composed of a tugboat, a towline, and a platform, is vulnerable to external environmental disturbances and inherent internal uncertainties. As a result, the actual towing path may deviate from the initially planned route without a good controller. This is especially the case when the system is under specific perturbation, which increases the difficulty of control [9]. Because the main risk comes from the off-course, how to keep the towing system navigating on the set path under those internal/external disturbances is crucial.

For the towing system of cylindrical drilling platform modeling, many scholars built the model based on MMG model developed by Maneuvering Modeling Group. The researches mainly focused on analyzing and controlling the stability of the towing system. Yasukawa et al. [10] found that a towing system is unstable when a crosswind is weak, and the towing system is less stable when the windboard angle is gradually increased. Fang and Ju [11] developed a nonlinear mathematical model that takes into consideration the seakeeping and maneuverability of the ship as well as the influence of wind, simulated the motion characteristics of ships in random waves, and studied the dynamic stability of the towing system in waves. Eik and Marchenko [12] used 1:40 ship physical model for towing experiment under different ice conditions to assess the risk of iceberg towing, and collected and analyzed the motion data of the iceberg. Huang [13] proposed a quantitative analysis method for towing safety for ship towing system design. Fitriadhy et al. [14, 15] established a mathematical model for the motion stability of a towing system and analyzed the parameters of the tugboat, the towing point, and the autopilot. Teknologi et al. [16] introduced an asymmetric system model, which can effectively improve the towing performance of the tugboat. Gavassoni et al. [17] presented a two degree of freedom (DoF) model to study the heave and pitch dynamical response in free and forced vibration. Sinibaldi and Bulian [18] came up with a four DoF (surge/sway/yaw/roll) model to analyze nonlinear towing dynamics.

For autonomous control of cylindrical drilling platform, to our knowledge, little has done on the path following control of the towing system, especially in the presence of environmental disturbances and possibly large modeling uncertainties. However, intelligent control methods widely applied to the intelligent ships bring us inspiration on autonomous control of the towing system. Ashrafiuon et al. [19] proposed a sliding-mode control law for trajectory tracking of underactuated autonomous surface vessels, which guarantees position tracking while the rotational motion remains bounded. Fahimi and Kleeck [20] designed a nonlinear trajectory-tracking controller for marine unmanned surface vessels using a nonlinear robust model-based sliding mode approach. Zhang et al. [21] presented adaptive neural path-following control for underactuated ships in fields of marine practice. Fossen et al. [22] came up with a nonlinear adaptive path following controller that compensates for drift forces through vehicle sideslip. Do [23] designed a global robust adaptive path-tracking controllers for underactuated ships. Zhang et al. [24] used a closed loop gain shaping algorithm combined with a linear reduction of backstepping for ship course keeping control. Paliotta et al. [25] presented a control strategy based on the input-output feedback linearization method for path following of underactuated marine vehicles. Those work show that traditional control methods often become insufficient when requiring a high level of control performance, especially under disturbances and uncertainties. Considering the similar complexity of the towing system to the above work, we propose to use Linear Active Disturbance Rejection Control (LADRC).

The LADRC is a linear version of the active disturbance rejection control (ADRC) concept, originally developed by Han [26] and Gao [27], inherent in the simplicity of Proportional-Integral-Derivative (PID) controller, but with better disturbance rejection ability. In ADRC, the internal dynamics and the external disturbances can be estimated by using an extended state observer (ESO). The dynamic compensation using state error feedback in each sampling period reduces the entire system to an approximate integrator chain. Nowadays, ADRC has attracted much attention in the field of control engineering [28, 29, 30, 31, 32, 33, 34].

In this paper, we built a three DoF dynamic model of a towing system in the wind and current environment. A LADRC based path following controller is designed to assure the towing system navigating on the safe route despite the nonlinear characteristics and large inertia within the system as well as the disturbances in the nautical environment. We then conducted simulation studies to validate and assess the feasibility of the established model, as well as the proposed control method.

The remainder of this paper is organized as follows. Section 2 describes the mathematical model of the towing system under environmental disturbances. Section 3 focuses on designing the LADRC based trajectory tracking controller. Simulation results are reported and discussed in Section 4. Section 5 concludes the paper.

## 2. Towing system modeling

In this section, we introduce a three DoF dynamic model of the towing system based on the MMG model and a catenary model. Specifically, the tugboat is affected by the hydrodynamic force, the propeller thrust, the rudder force and the force of the towline and their corresponding moments. The towed cylindrical drilling platform are affected by the hydrodynamic force and the force of the towline and their moments. Besides, the impact of external disturbance, such as the wind and current, as well as internal perturbation are taken into consideration.

### *2.1. Dynamic model of towing system*

#### *2.1.1. Coordinate system*

As shown in Fig.1, earth-fixed coordinate system $OXY$, tugboat coordinate system $o_1x_1y_1$ and cylindrical drilling platform coordinate system $o_2x_2y_2$ are adopted in the modeling process, and $o_1x_1y_1$ and $o_2x_2y_2$ are collectively called ship coordinate system. The $o_1x_1y_1$ is fixed to the tugboat with the origin at its center of gravity $(X_1, Y_1)$, $x_1$ and $y_1$ pointing to the forward and the starboard, respectively. Similarly, $o_2x_2y_2$ is fixed to the cylindrical drilling platform, with origin at its center of gravity $(X_2, Y_2)$, $x_2$ pointing to the connection point between the platform and the towline, and $y_2$ pointing to the starboard, respectively. The distances between two origins and the corresponding connection points are denoted by the half-length of the tugboat and the radius of the cylindrical drilling platform. $(X_{Li}, Y_{Li})$ denotes the towline connection point. $\psi_i$ is the drift angle. $V_i$ is ship speed. $\gamma$ is the angle of the towline direction in the earth-fixed coordinate system. $\omega_i$ is the towing angle between towline and the $x$-axis in the ship coordinate system. Here and after, the subscript $i \in 1, 2$ stands for the tugboat and the towed cylindrical drilling platform, respectively.

The relative position between the tugboat and the cylindrical drilling platform can be described by:

$$\begin{cases} X_{L1} = X_1 - L_1 \cos\psi_1 \\ Y_{L1} = Y_1 - L_1 \sin\psi_1 \\ X_{L2} = X_2 + L_2 \cos\psi_2 \\ Y_{L2} = Y_2 + L_2 \sin\psi_2 \\ \gamma = \arctan\left[\left(Y_{L2} - Y_{L1}\right) / \left(X_{L2} - X_{L1}\right)\right] \\ \omega_1 = \gamma - \psi_1 \\ \omega_2 = \gamma - \psi_2 \end{cases} \tag{1}$$

where $L_1$ and $L_2$ denote the half length of tugbaot and the radius of cylindrical drilling platform, respectively.

*2.1.2. Motion model of tugboat*

In this section, a three DoF tugboat motion model is developed based on the MMG model [35], ignoring the vertical motion:

$$\begin{cases} (m_i + m_{ix})\dot{u}_i - (m_i + m_{iy})v_i r_i = \sum F_{xi} \\ (m_i + m_{iy})\dot{v}_i - (m_i + m_{ix})u_i r_i = \sum F_{yi} \\ (I_{izz} + J_{izz})\dot{r}_i = \sum N_i \end{cases} \tag{2}$$

where $m$, $m_x$ and $m_y$ denote the mass and its added value in different directions. $I_{zz}$ and $J_{zz}$ represent the inertia moment and added value, respectively. $F_x$ and $F_y$ are the component force acting on the system in $x$ and $y$ direction respectively. $N$ is the corresponding moment. $u$ and $v$ are the speed in $x$ and $y$ direction respectively. $r$ is the angular velocity of turning.

*2.1.3. Mechanical model of towline*

Ignoring the vertical difference between the towed points on the tugboat and the platform, the catenary model can be established by considering the towing resistance and elasticity of the towline:

$$\begin{cases} F_T = \left(H_D - 2\frac{F_T}{\omega}sh^{-1}\left(\frac{\sigma L_R/2}{F_T}\right)\right)\frac{EA}{L_R} \\ R_L = 1.224\frac{SdV_i{}^2}{10^4}\left[1 + \frac{1.122}{10^4 F_T}\left(\frac{S}{10^3}\right)^2\right] \end{cases} \tag{3}$$

where $F_T$ is the component of the towline tension in the horizontal plane. $H_D$ is the horizontal distance between the two ends of the towline. $\sigma$ is the weight of the towline per unit length. $L_R$ is the length of the towline. $E$ is the Young's modulus of the towline. $A$ is the cross-sectional area of the streame. $R_L$ is the resistance of the rope. $d$ is the diameter of the towline. And $S$ is the length of the towline suspended into the water.

*2.2. Disturbing dynamic model*

The environmental disturbances such as wind and current on the towing safety, especially in restricted waters, dramatically increases the safety risk of the towing system. In general, the wind will cause severe turbulence in the towing system, while the current will lead the whole system to shift.

*2.2.1. Wind*

The wind is assumed to be a constant wind with fixed speed and direction, which generally can be modelled as follows:

$$\begin{cases} X_{windi} = \frac{1}{2}\rho_a A_{fi} V_{Ri}^2 C_{xi} L_i^2 \\ Y_{windi} = \frac{1}{2}\rho_a A_{si} V_{Ri}^2 C_{yi} L_i^2 \\ N_{wind} = Y_{windi} H_{LMi} \end{cases} \tag{4}$$

where $\rho_a$ denotes air density. $V_R$ is relative wind speed. $A_f$ and $A_s$ denote the orthographic area and side projection area of the ship structure above the ship's waterline, respectively. $C_x$ and $C_y$ are the wind coefficient in $x$ and $y$ direction in the ship coordinate system, relating to the relative wind direction and the shape of ships. $H_{LM}$ is the position of the wind action point. Here, we set $H_{LM}$ to the half of $L$.

*2.2.2. Current*

The effect of current acting on the ship is reflected by the relative current speed, which can be expressed by:

$$\begin{cases} u_{ri} = u_i + u_c \\ v_{ri} = v_i + v_c \end{cases} \tag{5}$$

where $u_r$ and $u_r$ are the speed related to the current in $x$ and $y$ direction in the ship coordinate system, respectively. $u_c$ and $u_c$ are the current speed in $x$ and $y$ direction, respectively.

## 3. LADRC based path following control

*3.1. Guidance law*

By taking into consideration errors between the sailing direction of the towing system (In this paper, we consider the actuator of the towing system, i.e., tugboat) and the desired direction, as well as the distance between the tugboat and the desired path, we establish the path following error based on the method of cross track error and parallax [36]. Fig. 2 shows the path guidance scheme. The calculation method of path following error is described below.

In Fig. 2, $(x_r(i), y_r(i))$ and $(x_r(i-1), y_r(i-1))$ denote the current and former desired target point, respectively. And $(x(t), y(t))$ stands for the current position of the tugboat.

We define:

$$\begin{cases} \Delta x = x_r(i) - x_r(i-1) \\ \Delta y = y_r(i) - y_r(i-1) \\ \hat{x} = x_r(i) - x(t) \\ \hat{y} = y_r(i) - y(t) \end{cases} \tag{6}$$

The path following error and the desired heading direction of tugboat are described as:

$$\begin{cases} \Delta d = (\hat{x}\Delta y - \hat{y}\Delta x)/\sqrt{\Delta x^2 + \Delta y^2} \\ \varphi_r(t) = tan(\hat{y}/\hat{x}) \end{cases} \tag{7}$$

The path following error can be expressed as:

$$\varphi(t) \ = \varphi_r(t) \ + k\Delta d \tag{8}$$

where $k$ denotes the weighted coefficient. $\varphi(t)$ denotes the current heading angle of the tugboat. Then, the path following problem of the towing system is transformed into the heading direction tracking problem.

### 3.2. Controller design

By the steps described in Section 3.1, the path following problem is transformed into the cross-track error tracking problem. Herein, we design the tracking controller based on LADRC.

According to the dynamic model of the towing system, the second order of rudder angle $\delta$ can be simplified as:

$$\ddot{\delta} = -a_1\dot{\delta} - a_2\delta + \omega_{drt} + bu, \tag{9}$$

where $\delta$ is the rudder angle, $u$ is the input and $\omega_{drt}$ denotes the external disturbance. $a_1$, $a_2$ and $b$ denote system parameters.

Then, Eq. (9) can be rewritten as:

$$\ddot{\delta} = -a_1\dot{\delta} - a_2\delta + \omega_{drt} + (b - b_0)u + b_0u = f\left(t, \delta, \dot{\delta}, \omega_{drt}\right) + b_0u \tag{10}$$

where $f\left(t, \delta, \dot{\delta}, \omega_{drt}\right) = -a_1\dot{\delta} - a_2\delta + \omega_{drt} + (b - b_0)\,u$ is the total disturbances, including internal disturbances $-a_1\dot{\delta} - a_2\delta + (b - b_0)\,u$ and the external disturbances $\omega_{drt}$ . $b_0$ is the estimation of $b$.

Let

$$\begin{cases} \dot{x}_1 = x_2 \\ \dot{x}_2 = x_3 + b_0u \\ \dot{x}_3 = h \\ \delta = x_1 \end{cases} \tag{11}$$

where $h = \dot{f}\left(t, \delta, \dot{\delta}, \omega\right)$.

Then, Eq. (10) can be rewritten by considering extended state space:

$$\begin{cases} \dot{x} = \boldsymbol{A}x + \boldsymbol{B}u + \boldsymbol{E}h \\ \delta = \boldsymbol{C}x \end{cases} \tag{12}$$

where $\boldsymbol{A} = \begin{bmatrix} 0 & 1 & 0 \\ 0 & 0 & 1 \\ 0 & 0 & 0 \end{bmatrix}$, $\boldsymbol{B} = \begin{bmatrix} 0 \\ b \\ 0 \end{bmatrix}$, $\boldsymbol{C} = \begin{bmatrix} 1 & 0 & 0 \end{bmatrix}$, $\boldsymbol{E} = \begin{bmatrix} 0 \\ 0 \\ 1 \end{bmatrix}$.

Then the ESO of the towing system is constructed as:

$$\begin{cases} \dot{z} = \boldsymbol{A}z + \boldsymbol{B}u + \boldsymbol{L}\left(\delta - \hat{\delta}\right) \\ \hat{\delta} = \boldsymbol{C}z \end{cases} \tag{13}$$

where $\boldsymbol{L} = [\beta_1, \beta_2, \beta_3]$ is the observer gain vector, which are parameterized as $\beta_1 = 3\omega_o, \beta_2 = 3\omega_o^2, \beta_3 = \omega_o^3$, $\omega_o$ is the only tuning parameter, stands for the observer bandwidth. If the bandwidth is well tuned, the observer states $z$ excellent tracks the states $x$. With the ESO properly designed, the current rudder angle $\delta$ of the towing system, and its changing rate $\dot{\delta}$, as well as the total disturbance $f$ can be well estimated. Moreover, through the dynamic compensation of error state feedback control law, the path following control of the towing system is realized.

Let

$$u = \frac{-z_3 + u_0}{b_0} \tag{14}$$

Ignoring the estimation error of $z_3$, the system model is reduced as:

$$\ddot{\delta} = f - z_3 + b_0 u \approx u_0 \tag{15}$$

The feedback control law is illustrated as:

$$u_0 = k_p(r - z_1) + k_d(\dot{r} - z_2) \tag{16}$$

According to [37] and [38], in the face of large environmental disturbances and internal dynamic uncertainties, estimation, and path following errors are shown to be bound, with their bounds monotonously decreasing with their respective bandwidths. The estimation error of the ESO is upper bounded and its upper bound value decreases monotonously with the bandwidth of the observer, whereas the tracking error of LADRC is upper bounded and the upper bound value decreases monotonously with the bandwidth of the controller.

### *3.3. Robustness analysis*

The Monte Carlo (MC) method [39] uses a given system model (i.e., the towing system) and introduces statistical uncertainties (internal dynamics and external disturbances) into the model. These disturbances and uncertainties are categorized for the analysis by using a uniform distribution. That is, the towline tension of the towing system varies by -20% to +20% during 2000 s to 3000 s, the speed of current along $X$ and $Y$ direction changes from -1 m/s to 1 m/s during 2500 s to 2700 s, the speed of constant crosswind along $X$ and $Y$-axis changes from -10 m/s to 10 m/s during 2200 s to 2400 s. The MC simulation results with 200 sets of stochastic parameters during 2000 s to 4000 s (all disturbances occur in this period) are shown in Fig. 3.

From Fig. 3, we observe that the path following errors for the desired path with all the parameter sets are bounded, which indicates that the control system is robust.

## 4. Simulation analysis

### *4.1. Towing system settings*

The simulation experiments are carried out aiming at a specific type of the tugboat and the towed cylindrical drilling platform with the physical parameters shown in Table 1 and Table 2, respectively.

Considering that the tonnage of the towed cylindrical drilling platform is large, the towline adopts a suitable steel cable to ensure towing safety. The dragging parameters are shown in Table 3.

In the simulation, the tugboat is driven by the propeller thrust, its direction control is achieved by adjusting the rudder angle $\delta$. Limitations for the rudder angle and the steering speed should also meet $|\delta| \leq 35°$ and $\left|\dot{\delta}\right| \leq 3°/s$. The initial velocity of the towing system is set to 2.57 m/s (5 kn).

### *4.2. Simulation examples*

#### *4.2.1. Model validation*

The simulation is designed to validate the established model, as well as test the effects of environmental disturbances and inherent uncertainties acting on the towing system. Considering the most unfavorable factors in the maneuvering process, e.g., the crosswind, cross flow, et al. Thus, the simulation environment is set as follows: the whole simulation time is 8000 s. The initial heading of the tugboat and the towed cylindrical drilling platform is configured to 90°. From 2000 s to 3000 s, the constant wind of speed 20 m/s coming from left abeam is added. During 4000 s to 5000 s, the constant current of speed 2 m/s coming from left abeam is applied. The internal perturbation of the towline is added between 6000 s and 7000 s, which is realized by increasing the towline force to 120%. The simulation results are shown in Fig.4.

As shown in Fig.4, before 2000 s, the towing system gradually reaches equilibrium due to the hydrodynamic force, the propeller thrust, the rudder force, the towline tension and their corresponding moments achieve balance. The speed of the towing system is stabilized at 4.58 m/s. There is no speed and motion in the $Y$-direction as all these force are affected in $X$-direction and its corresponding moment are 0.

At t = 2000 s, the 20 m/s constant wind from left abeam appears. It can be observed from Fig.4 (b), the $Y$-axis speed of both tugboat and platform increases from 0 to 0.1 m/s and the off-course distance to the leeward direction increase gradually. Due to the hug difference of ship shapes, the speed and position changes of the tugboat and the platform have the phase and amplitude differences, which become more distinguished after the wind. This indicates that the tugboat is more sensitive to the wind than the cylindrical drilling platform.

The current effect is exposed from 4000 s to 5000 s. Compared with the wind, the speed increase with a more significant increasing rate. It is revealed from fig.4 (a) that the towing system has an evident motion toward its right abeam and the lateral drift distance is up to 1800 m, which is almost 18 times that caused by the wind. As shown in Fig.4 (c), the speed of tugboat and platform in the current direction are increased to 2 m/s.

The period from 6000 s to 7000 s experienced an impact caused by internal perturbation of the towline tension. As the towline tension force is same as the heading of the towing system so that only its x-direction speed only slightly fluctuated. The speed of tugboat variates from -0.2 m/s to 0.2 m/s, and from the perspective of the cylindrical drilling platform, its speed oscillates from -0.03 m/s to 0.03 m/s. The corresponding off course deviation, in this case, can be neglected.

*4.2.2. Path following simulation*

In real applications, offshore drilling platform towing is always pre-planned and the towing operating area is usually reserved for towing operations. Therefore, the experimental path is designed as a polyline in the horizontal plane. The first straight line is with a starting point (0 m, 0 m) and an ending point (5000 m, 0 m) ; the second straight-line stars from the ending point of the first line, i.e. (5000 m, 0 m), points at (10000 m, 1000 m) m.

To verify the path following control performance, both the LADRC and the traditional PID controllers are applied for path following under various disturbance conditions, including no disturbance, wind disturbances, current disturbance, towline tension disturbance, and all disturbances, which are described as follows:

1) No disturbance.

2) Wind disturbances: the constant lateral wind of speed 20 m/s coming from left abeam is added at t = 2500 s, and the duration time is 100 s.

3) Current disturbance: at t = 2500 s, the current of speed 2 m/s coming from the left abeam is add, and lasts 100 s.

4) Towline tension disturbances: the towline tension of the towing system increases by +20% during 2500 s to 2600 s.

5) All disturbances: includes all above-mentioned disturbances and parametric uncertainties.

In order to measure the path following effects, the control output at the $i$-th sampling time point is denoted by $u(i)$, the distance between the designed position and the actual position of the $i$-th sampling time is denoted by $l(i)$, and the maximum sampling time is defined by $N$. Then, the energy consumption $s$, the maximum error by $e_{\max}^{pos}$, the average error by $e_{ave}^{pos}$, and the error variance by $\sigma^{pos}$ are represented as follows:

$$s = \sum_{i=1}^{N} |u(i) - u(i-1)|$$

$$e_{\max}^{pos} = \max_{i} |l(i)|$$

$$e_{ave}^{pos} = \frac{1}{N} \sum_{i=1}^{N} |l(i)|$$

$$\sigma^{pos} = \sqrt{\frac{1}{N} \sum_{i=1}^{N} l(i)^2}$$

LADRC are tuned as $\omega_o = 3$, $b_0 = 0.015$, and $\omega_c = 0.2$. Comparing the performance and robustness of the PID control systems by integral of time-weighted absolute error (ITAE) index [40], PID controllers are tuned as $k_p = 5$, $k_i = 1$, and $k_d = 0.1$. A comparison between LADRC and PID controllers by applying these five disturbance conditions is presented in Fig. 5 - Fig. 9. The position errors of ADRC and PID controllers are listed in Table 4 - Table 5.

As represented in Fig. 5 (a) and (b), we can observe that both LADRC and PID controllers can follow the reference path well under the condition of no disturbances. From inset in Fig. 5 (a), we can see that the overall tracking error of LADRC is smaller than PID controller. As show in Table 4 and Table 5, the maximum path following error $e^{pos}_{\max}$ and the average path folowing error $e^{pos}_{ave}$ of LADRC are smaller than that of PID, the total energy consumption $s$ of LADRC is only 40Especially at the turning stage, the output of the PID controller approaches saturated, while the LADRC shows better response rates and smaller overshoot. The smaller value of the error variance $\sigma^{pos}$ shows more path following stability of LADRC.

In the case of wind disturbances as shown in Fig. 6 (a) and (b), LADRC and PID controllers also follow the desired path well. However, the path following effect using the PID controller is worse than the one using the LADRC, which is revealed by the inset in Fig. 6 (a). The detailed comparison of position errors is listed in Table 4 and Table 5, showing that $e^{pos}_{\max}$, $e^{pos}_{ave}$ and $s$ of LADRC are smaller that PID controller. In general, the LADRC can tackle the influence of wind more efficiently leading to a better path following. Besides, we can see that the PID controller produces a more extended period of overshoot during the wind.

From the simulation results of Fig. 7 (a) and (b), we can observe that the current disturbances have a more significant influence on the path following than the results with the wind disturbances, using the same controllers. This also coincides the previous results shown in Fig.4. For the PID controller, 7 (b) also shows that the short-term control output starts saturating after the current perturbation was applied. A further simulation shows that the output of the PID controller is saturated and the system diverges when the speed of current increases to 2.5 m/s. In contrary, the LADRC can still track the desired path when the current speed increases to 2.5 m/s, showing strong anti-disturbance performance and robustness.

In Fig. 8 (a) and (b), we observe that the tension disturbance have the least influence on the path following control of the towing system. In addition to the slight fluctuations in the controller output immediately after the disturbance is added, the control criteria are similar to the situation with no disturbance. On energy consumption, the control performance of the LADRC is better than that of the PID controller, reflected by $s$ listed in Table 4.

When the towing system is affected by both internal uncertainties and external disturbances as shown in Fig. 9 (a) and (b), there exists both external disturbances and strong coupling within the system. The LADRC can detect the internal and external disturbances through ESO and perform dynamic compensation to achieve precise path following control. As shown in Table 4 and Table 5, the control criteria under all disturbances are the worst among all tests. Compared with the PID controller, LADRC achieves better control precision and robustness.

Compared with the position error of the tugboat shown in Table 4, all the control criteria of the cylindrical drilling platform, such as $e^{pos}_{\max}$, $e^{pos}_{ave}$ and $\sigma^{pos}$, show smalller differences, as listed in Table 5. The reason is that the tugboat that drags the cylindrical drilling platform to the target area is considered as the control object.

Compared with single disturbances, the towline tension disturbances have little influence on the control performances, especially for the position errors listed in Table 4 and Table 5. Moreover, the position error of the current disturbance is the largest. Therefore, we may conclude that current disturbance is the primary factor affecting the precise path following control of the towing system.

## 5. Conclusion

In this paper, we first developed a three DoF dynamic model of the towing system under various disturbance conditions based on the MMG model and the catenary model. Then, we proposed a control strategy based on LADRC for path following control of the towing system. The control strategy was designed to tackle inner uncertainties and external disturbances by compensating the disturbance estimated by an ESO in each sampling period. The simulation results clearly show that the dynamic model can accurately describe the characteristics of the practical towing system under various disturbances, and the proposed method achieves more desirable control performance than the traditional PID controller.

The towing system of cylindrical drilling platform is a complicated nonlinear system. It has been intricate to calculate and analyze the internal dynamics of the system. Besides, there are many parameters and tuning difficulties in the design of the ADRC. For future work, we plan to simplify the control tuning strategy, improve the control precision, and investigate higher precision path following for potential practical engineering applications.

[1] Nersesian R. Energy for the 21st century: a comprehensive guide to conventional and alternative sources. London: Routledge; 2014.

[2] Trenchard H, Perc M. Energy saving mechanisms, collective behavior and the variation range hypothesis in biological systems: A review, BioSystems. 2016; 147: 40-66. https://doi.org/10.1016/j.biosystems.2016.05.010.

[3] Chinnese State Council. Energy development action plan (2014-2020), http://www.gov.cn/zhengce/content/2014-11/19/content_9222.htm; 2014.

[4] Pinder D. Offshore oil and gas: global resource knowledge and technological change. Ocean Coastal Manage 2001; 44(9-10): 579-600. https://doi.org/10.1016/S0964-5691(01)00070-9.

[5] Major F, Syvertsen K, Aarsnes JV. Significant benefits with a cylindrical hull for FPSO, drilling, LNG, and offshore power plant applications. APPEA J 2009; 48(2): 464-464. https://doi.org/10.1071/AJ07054.

[6] Akyuz E., Celik M. Utilisation of cognitive map in modelling human error in marine accident analysis and prevention. Saf Sci 2014; 70: 19-28. https://doi.org/10.1016/j.ssci.2014.05.004.

[7] Borkowski P. Inference engine in an intelligent ship course-keeping system. Comput Intell Neurosci 2017; 2561383. https://doi.org/10.1155/2017/2561383.

[8] Liu CG, Chu XM, Xie S. Review and prospect of ship intelligence. Ship Eng 2016; 38(3): 77-84.

[9] Fossen TI. Handbook of marine craft hydrodynamics and motion control. New Jersey: John Wiley & Sons; 2011.

[10] Yasukawa H, Hirata N, Tanaka K, Hashizume Y, Yamada R. Circulation Water tunnel tests on slewing motion of a towed ship in wind. J Mar Sci Technol. 2007; 6:323-329. https://doi.org/10.2534/jjasnaoe.6.323,

[11] Fang M C, Ju J H. The dynamic simulations of the ship towing system in random waves. Mar Technol. 2009; 46(2):107-115.

[12] Eik K, Marchenko A. Model tests of iceberg towing. Cold Reg Sci Technol. 2010; 61(1):13-28. https://doi.org/10.1016/j.coldregions.2009.12.002.

[13] Huang X B, Huang X L. Safety analysis and decision making methodology in ship towing system design. Apply Mech Materials. 2012; 201-202:1013-1016. https://doi.org/10.4028/www.scientific.net/AMM.201-202.1013.

[14] Ahmad F, Hironori Y. Course stability of a ship towing system. Ship Technol Research, 2011(58):4-23.

[15] Fitriadhy A, Yasukawa H, Koh KK. Course stability of a ship towing system in wind. Ocean Eng. 2013; 64: 135-145. https://doi.org/10.1016/j.oceaneng.2013.02.001

[16] Fitriadhy A, Yasukawa H, Yoneda T, Koh KK, Maimun A. Analysis of an asymmetrical bridle towline model to stabilise towing performance of a towed ship. Jurnal Teknologi, 2013, 662: 2180-3722. https://doi.org/10.11113/jt.v66.2502

[17] Gavassoni E, Gonalves PB, Roehl DM. Nonlinear vibration modes and instability of a conceptual model of a spar platform. Nonlinear Dyn. 2014; 76(1): 809-826. https://doi.org/10.1007/s11071-013-1171-6.

[18] Sinibaldi MK, Bulian G. Towing simulation in wind through a nonlinear 4-DOF model: Bifurcation analysis and occurrence of fishtailing. Ocean Eng. 2014; 88: 366-392. https://doi.org/10.1016/j.oceaneng.2014.06.007

[19] Ashrafiuon H, Muske KR, McNinch LC, Soltan RA. Sliding-mode tracking control of surface vessels. IEEE Trans Ind Electron. 2008; 55(11): 4004-4012. https://doi.org/10.1109/TIE.2008.2005933.

[20] Fahimi F, Kleeck CV. Alternative trajectory-tracking control approach for marine surface vessels with experimental verification. Robotica. 2013; 31(1): 25-33. https://doi.org/10.1017/S0263574712000070.

[21] Zhang GQ, Zhang XK, Zheng YF. Adaptive neural path-following control for underactuated ships in fields of marine practice. Ocean Eng. 2015; 104: 558-567. https://doi.org/10.1016/j.oceaneng.2015.05.013.

[22] Fossen TI, Pettersen KY, Galeazzi R. Line-of-sight path following for dubins paths with adaptive sideslip compensation of drift forces. IEEE Trans Control Syst Technol. 2015; 23(2): 820-827. https://doi.org/10.1109/TCST.2014.2338354.

[23] Do KD. Global path-following control of underactuated ships under deterministic and stochastic sea loads. Robotica. 2016; 34(11): 2566-2591. https://doi.org/10.1017/S0263574715000211.

[24] Zhang XK, Zhang Q, Ren HX, Yang GP. Linear reduction of backstepping algorithm based on nonlinear decoration for ship course-keeping control system. Ocean Eng. 2018; 147: 18. https://doi.org/10.1016/j.oceaneng.2017.10.017.

[25] Paliotta C, Lefeber E, Pettersen KY, Pinto J, Costa M. Trajectory tracking and path following for underactuated marine vehicles. IEEE Trans Control Syst Technol. 2018; 1-15. https://doi.org/10.1109/TCST.2018.2834518.

[26] Han J. From PID to active disturbance rejection control. IEEE Trans Ind Electron. 2009; 56(3): 900-906. https://doi.org/10.1109/TIE.2008.2011621.

[27] Gao Z. Scaling and bandwidth-parameterization based controller tuning. Proceedings of the American control conference; 2003 Jun 4-6; Denver, Colorado, USA. Piscataway: IEEE; 2004.

[28] Gao BW, Shao JP, Yang XD. A compound control strategy combining velocity compensation with ADRC of electro-hydraulic position servo control system. ISA Trans. 2014; 53(6): 1910-1918. https://doi.org/10.1016/j.isatra.2014.06.011.

[29] Zhou XY, Gao H, Zhao BL, Zhao LB. A GA-based parameters tuning method for an ADRC controller of ISP for aerial remote sensing applications. ISA Trans. 2018; 81, 318-328. https://doi.org/10.1016/j.isatra.2018.08.001

[30] Tao J, Sun QL, Sun H, Chen ZQ, Dehmer M, Sun MW. Dynamic modeling and trajectory tracking control of parafoil system in wind environments. IEEE-ASME Trans Mech. 2017; 22(6): 2736-2745. https://doi.org/10.1109/TMECH.2017.2766882.

[31] Pawar SN., Chile RH, Patre BM. Modified reduced order observer based linear active disturbance rejection control for TITO systems. ISA Trans. 2017; 71, 480-494. https://doi.org/10.1016/j.isatra.2017.07.026

[32] Tao J, Liang W, Sun QL, Luo SZ, Chen ZQ, Tan PL. He YP. Modeling and control of a powered parafoil in wind and rain environments. IEEE Trans Aerosp Electron Syst. 2017; 53(4): 1642-1659. https://doi.org/10.1109/TAES.2017.2667838.

[33] Tao J, Sun QL, Tan PL, Chen ZQ, He YP. Autonomous homing control of a powered parafoil with insufficient altitude. ISA Trans. 2016; 65: 516-524. https://doi.org/10.1016/j.isatra.2016.08.016.

[34] Tian JY, Zhang SF, Zhang YH, Li T. Active disturbance rejection control based robust output feedback autopilot design for airbreathing hypersonic vehicles. ISA Trans. 2018; 74, 45-59. https://doi.org/10.1016/j.isatra.2018.01.002

[35] Yoshimura Y. Mathematical model for manoeuvring ship motion (MMG Model). In Workshop on Mathematical Models for Operations involving Ship-Ship Interaction, pp. 1-6, 2005

[36] Kang Y, Hedrick JK. Linear tracking for a fixed-wing UAV using nonlinear model predictive control. IEEE Trans Control Syst Technol. 2009; 17(5): 1202-1210. https://doi.org/10.1109/TCST.2008.2004878.

[37] Zheng Q, Gaol LQ, Gao ZQ. On stability analysis of active disturbance rejection control for nonlinear time-varying plants with unknown dynamics. 46th IEEE Conference on Decision and Control; Dec 12-14, 2007; Louisiana, USA. Piscataway: IEEE; 2007. p. 3501-3506.

[38] Zheng Q, Dong L, Lee DH, Gao ZQ. Active disturbance rejection control for MEMS gyroscopes. American Control Conference; Jun 11-13, 2008; Seattle, Washington, USA. Piscataway: IEEE; 2008. p. 4425-4430.

[39] Doucet A, De Freitas N, Gordon N. An introduction to sequential Monte Carlo methods. New York: Springer; 2001.

[40] Martins FG. Tuning PID controllers using the ITAE criterion. Int J Eng Educn. 2005; 21(5): 867.

Table 1: Physical Parameters of tugboat

| Parameters | Length | Width | Displacement | Draught | Square factor |
|---|---|---|---|---|---|
| Values/Unites | 63.6 m | 16.4 m | 4522 t | 6.22 m | 0.692 |
| Parameters | Rudder area | Rudder height | Aspect ratio | Pitch | Propeller diameter |
| Values/Unites | 7.5 $m^2$ | 5 m | 1.7 | 5.2 m | 5 m |

Table 2: Physical Parameters of cylindrical drilling platform

| Parameters | Diameter | Draught | Tonnage | Square factor |
|---|---|---|---|---|
| Values/Unites | 86 m | 6.4 m | [illegible]000 t | 0.7854 |

Table 3: Physical Parameters of towline

| Parameters | Diameter | Reference quality | Tensile compression stiffness | Maximum load |
|---|---|---|---|---|
| Values/Unites | 54.6 mm | 12 kg$\cdot$ $m^{-1}$ | $9.2\times10^8$ N | 1800 kN |

Table 4: Position errors of tugboat

| Parameters | Conditions | s (Unitless) | $e^{pos}_{\max}$ (m) | $e^{pos}_{ave}$ (m) | $\sigma^{pos}$ (Unitless) |
|---|---|---|---|---|---|
| LADRC | No disturbance | 1.8339 | 4.8813 | 0.2720 | 0.3040 |
| | Atmospheric disturbances | 4.6907 | 5.4927 | 0.6086 | 5.0167 |
| | Current disturbance | 7.0027 | 69.0607 | 0.9298 | 21.2396 |
| | towline tension disturbances | 1.8714 | 5.3894 | 0.2717 | 0.2942 |
| | All disturbances | 8.1727 | 110.1416 | 1.5622 | 66.5513 |
| PID | No disturbance | 4.4556 | 6.9023 | 3.0873 | 19.3810 |
| | Atmospheric disturbances | 5.5718 | 27.8238 | 3.1243 | 20.1987 |
| | Current disturbance | 12.0760 | 32.4425 | 3.5679 | 52.0664 |
| | Towline tension disturbances | 4.3540 | 7.0365 | 3.0878 | 19.4180 |
| | All disturbances | 22.7363 | 153.1272 | 7.4504 | 806.5526 |

Table 5: Position errors of cylindrical drilling platform

| Parameters | Conditions | $e^{pos}_{\max}$ (m) | $e^{pos}_{ave}$ (m) | $\sigma^{pos}$ (Unitless) |
|---|---|---|---|---|
| LADRC | No disturbance | 289.8555 | 176.8532 | $4.3522\times10^4$ |
| | Atmospheric disturbances | 285.9481 | 178.6055 | $4.4390\times10^4$ |
| | Current disturbance | 288.5336 | 190.0993 | $4.7512\times10^4$ |
| | Towline tension disturbances | 288.7610 | 175.9806 | $4.3107\times10^4$ |
| | All disturbances | 328.0973 | 193.2258 | $5.2754\times10^4$ |
| PID | No disturbance | 310.8163 | 185.3600 | $4.8090\times10^4$ |
| | Atmospheric disturbances | 289.0504 | 177.1040 | $4.3678\times10^4$ |
| | Current disturbance | 326.9093 | 191.8426 | $5.1662\times10^4$ |
| | Towline tension disturbances | 309.9453 | 184.7290 | $4.7761\times10^4$ |
| | All disturbances | 378.2506 | 201.2743 | $7.8992\times10^4$ |

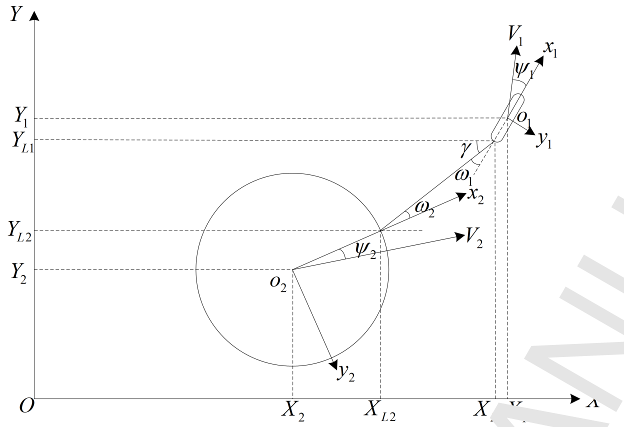

Figure 1: Coordinates system of towing system

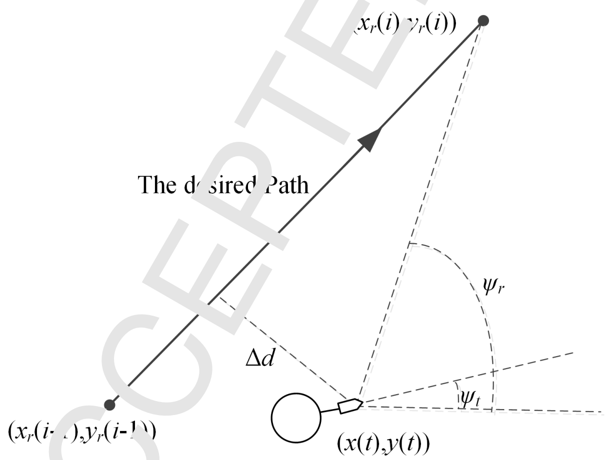

Figure 2: Path following scheme of towing system

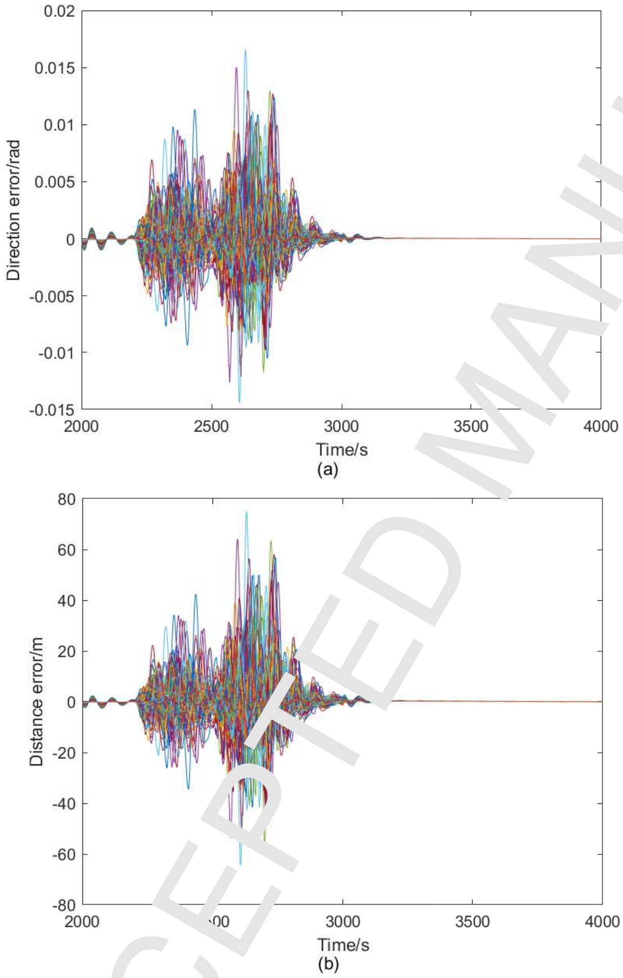


Figure 8. Simulation results based on LADRC with stochastic parameters; (a) Direction error; (b) Distance error.

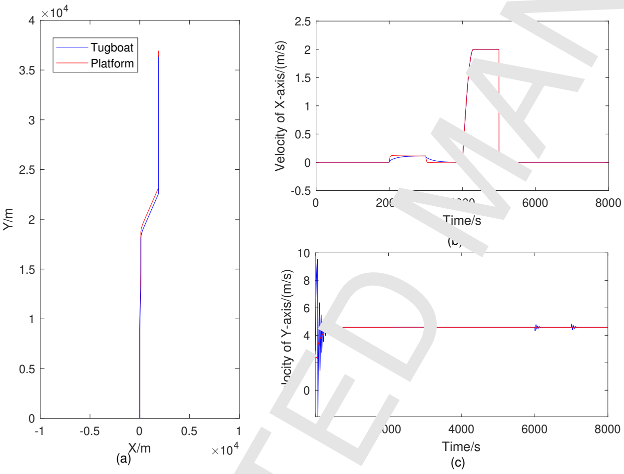


Figure 4: Motion simulation of towing system under disturbances and uncertainties; (a) The path of towing system, (b) Velocity of x-direction, (c) Velocity of y-direction.

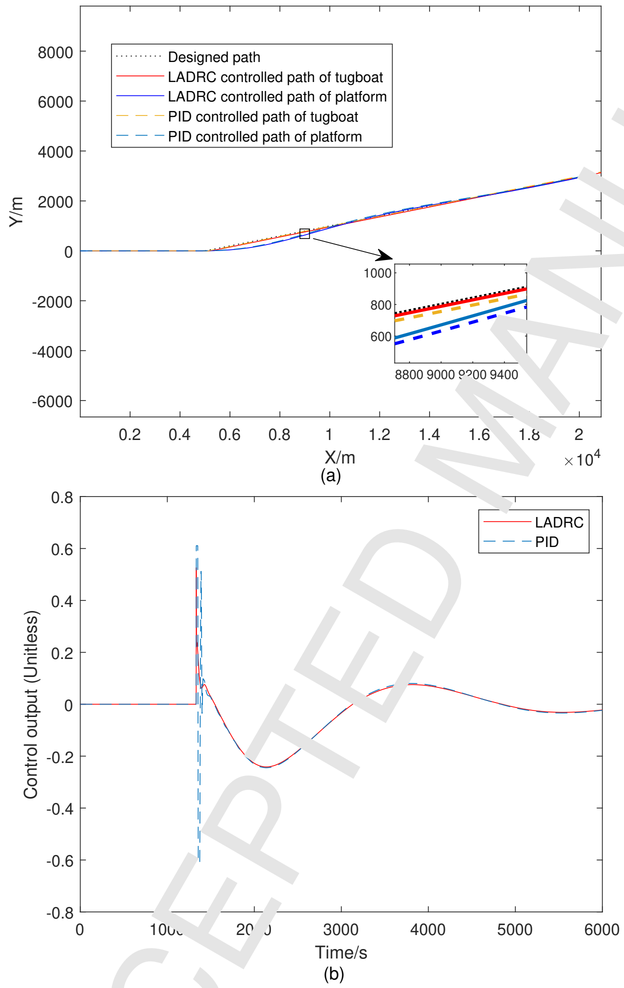


Figure 5: Path following control with no disturbance; (a) LADRC and PID controllded path following trajecroties, (b) Control outputs of LADRC and PID.

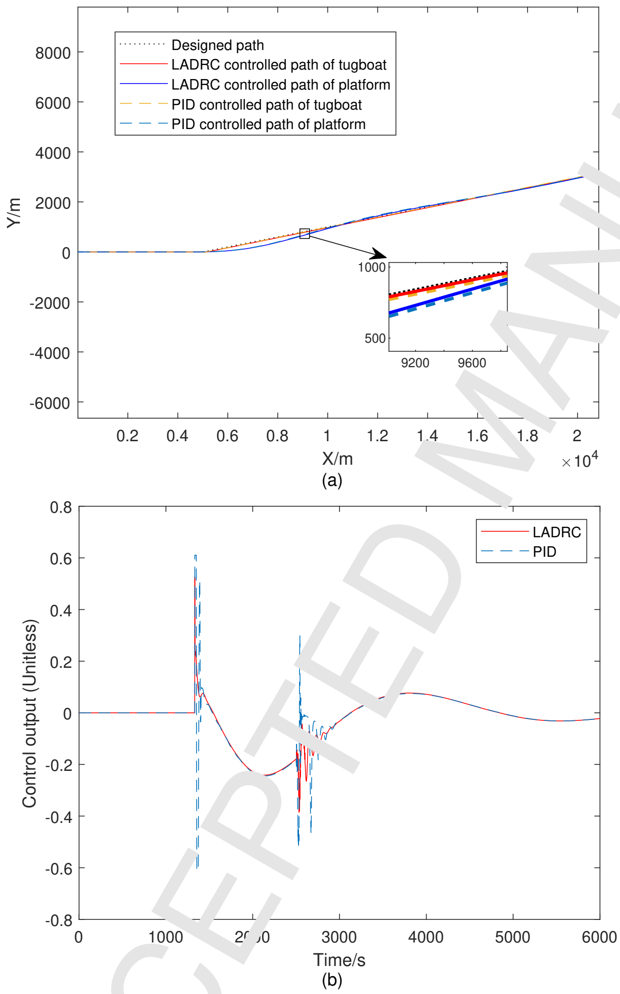


Figure 6. Path following control with wind disturbance; (a) LADRC and PID controllded path following trajecroties, (b) Control outputs of LADRC and PID.

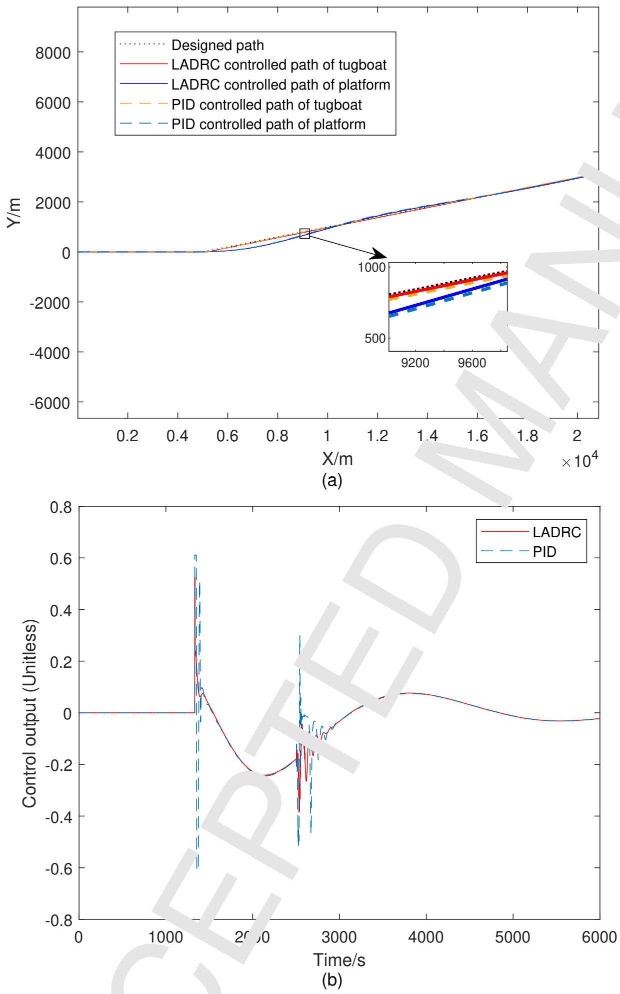


Figure 7: Path following control with current disturbance; (a) LADRC and PID controlled path following trajecroties, (b) Control outputs of LADRC and PID.

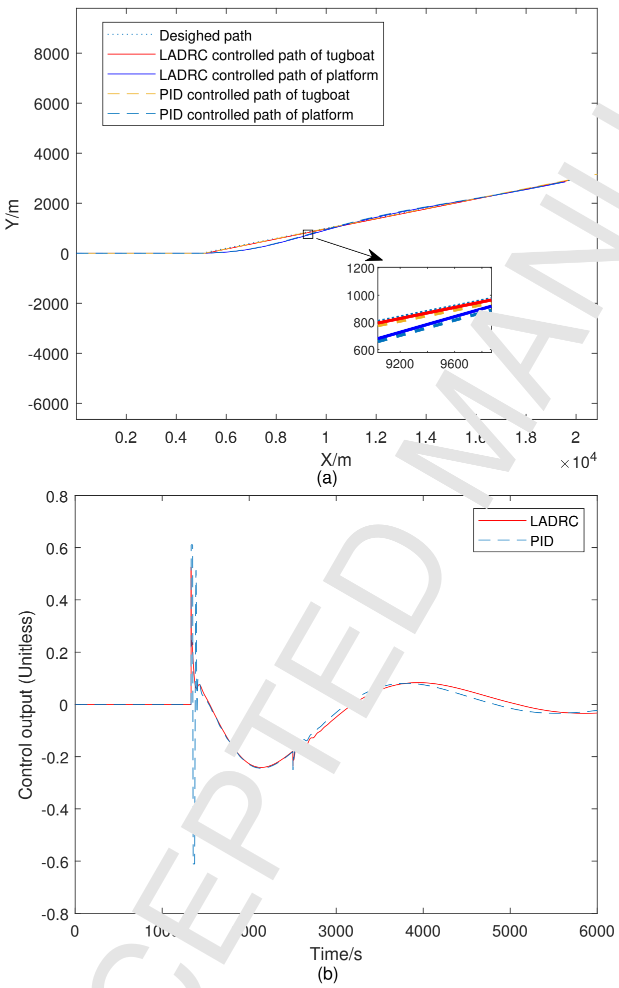


Figure 8: Path following control with tension disturbance; (a) LADRC and PID controlled path following trajecroties, (b) Control outputs of LADRC and PID.

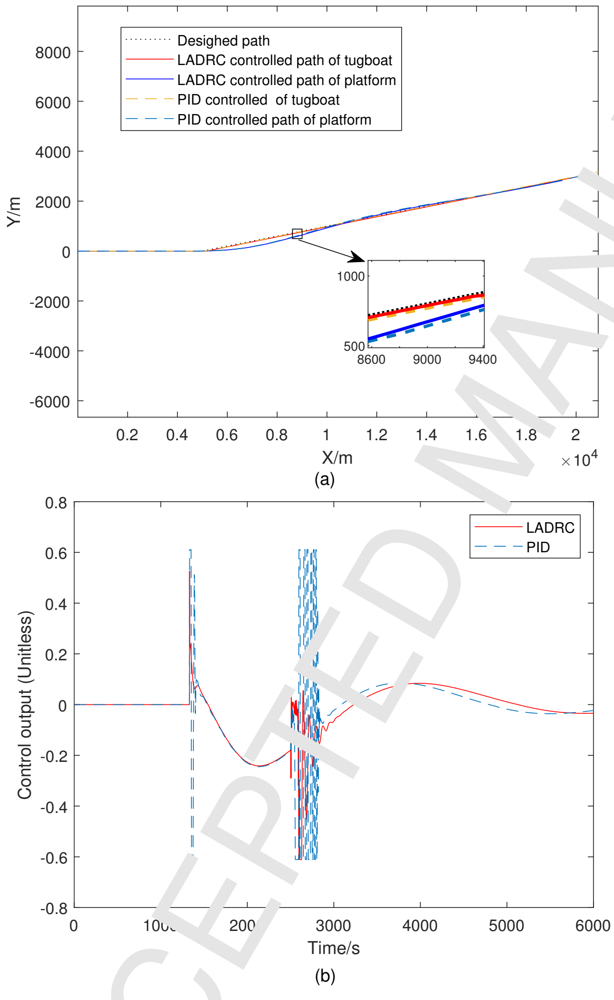


Figure 9: Path following control under all disturbances; (a) LADRC and PID controllded path following trajecroties, (b) Control outputs of LADRC and PID.

**Highlights:**

- Establishment and validation of the dynamic model for towing system under disturbances and uncertainties
- Design of linear active disturbance rejection control based path following controller for the towing system
- Linear active disturbance rejection control achieves more desirable tracking performance than traditional proportional–integral–derivative controller

## Conflict of interest statement

The authors whose names are listed in the paper certify that they have NO affiliations with or involvement in any organization or entity with any financial interest (such as honoraria; educational grants; participation in speakers' bureaus; membership, employment, consultancies, stock ownership, or other equity interest; and expert testimony or patent-licensing arrangements), or non-financial interest (such as personal or professional relationships, affiliations, knowledge or beliefs) in the subject matter or materials discussed in this manuscript.